43rd European Rotorcraft Forum, September 12–15, 2017, Milan, Italy

Paper ID 538

Experimental Evaluation of an Active Controlled L-Shaped Tab for Dynamic Stall Alleviation

A. Zanotti*, D. Grassi, G. Pisetta and G. Gibertini

Politecnico di Milano, Dipartimento di Scienze e Tecnologie Aerospaziali
Campus Bovisa, Via La Masa 34, 20156 Milano, Italy
*e-mail: alex.zanotti@polimi.it

Keywords: Dynamic Stall, Gurney Flap, Pitching Airfoil, Wind Tunnel.

Abstract

The present paper describes the experimental activity carried out to investigate the effectiveness of an active trailing edge L-shaped tab for deep dynamic stall control. Wind tunnel tests were performed on a NACA 23012 pitching airfoil in deep dynamic stall conditions. The L-shaped tab was designed to behave as a Gurney flap when deployed, as its end prong protrudes at the airfoil trailing edge, while in retracted position the tab behaves as a trailing edge flap. The active control of the deployment and retraction of the tab along the oscillating cycle was based on the use of micro pneumatic actuators guided by miniaturized servovalves. The results of unsteady pressure measurements carried out on the airfoil model midspan contour showed that important benefits for blade aerodynamic performance and structural integrity prevention could be achieved deploying the tab during the upstroke motion and retracting the tab during the downstroke. The main goal obtained by the active control system was a conspicuous increase of the net positive aerodynamic damping associated to the pitching moment, thus ensuring to avoid the risk of stall flutter occurrence. Moreover, the tab deployment in upstroke produces a conspicuous increase of lift corresponding to a higher level of available thrust very useful on the retrating side of a helicopter rotor. The retraction of the tab before the stall onset enables also to reduce the pitching moment peak with respect to the clean airfoil configuration. The present tests results illustrates that the tested L-shaped tab can be considered a very attractive device to be employed on helicopter rotr blades for dynamic stall control due to its easier integration at the trailing edge with respect to an active deployable Gurney flap.

Nomenclature

α	angle of attack [deg]
α_m	mean angle of attack [deg]
α_a	pitching oscillation amplitude [deg]
ω	circular frequency [rad/s]
a_2	two-dimensional aerodynamic damping coefficient
b	airfoil section model span [m]
c	airfoil section model chord [m]
C_L	lift coefficient
C_M	pitching moment coefficient about the airfoil quarter chord
C_p	pressure coefficient
f	oscillation frequency [Hz]
h	height of the deployed L-tab end prong below the trailing edge [m]
HES	Hall Effect Sensor
k	reduced frequency $= \pi f c/U_\infty$
M	Mach number
Re	Reynolds number
t	time [s]
U_∞	free-stream velocity [m/s]

1 Introduction

In the recent years, the strong demand of faster helicopters has spurred the attention of rotorcraft industry, academia and research centers to the design of active blades aimed to control the detrimental effects on helicopter performance produced by retreating blade dynamic stall [1, 2]. Of course, the evaluation of an effective active device suitable to be installed on a helicopter rotor blade represents a very challenging activity due to the severe requirements related to its integration and to the severe operative conditions of the helicopter flight envelope. Many attractive solutions for improving helicopter performance and alleviate the detrimental effects of dynamic stall were recently investigated as, for instance, the use of air-jet vortex generators [3], plasma actuators [4] or backflow flaps [5].

Among these studies, the use of an active deployable Gurney flap [6] on rotor blades [7] exhibits potential benefits for rotorcraft performance, as shown by numerical activities [8, 9, 10] and also supported by experiments carried out on pitching airfoils equipped with a Gurney flap in steady condition [11]. Nevertheless, the integration of an active Gurney flap on a rotor blade implicates important feasibility problems, related mainly to the very severe requirement to stow the deployable device together with the required actuation mechanism inside the airfoil at the blade trailing edge. Thus, a novel trailing edge L-shaped tab was investigated at Politecnico di Milano to overcome this limitation. Indeed, this tab, thanks to its design, exhibits the suitability to be installed in a easier way at the trailing edge region with respect to a deployable Gurney flap. Preliminary numerical [12] and experimental studies [13] carried out with the L-shaped tab in fixed positions showed very encouraging results for blade aerodynamic performance improvement. The effectiveness of an active controlled L-tab for dynamic stall control was firstly investigated using a preliminary set up in the activity described in Pisetta Master's thesis [14]. The present paper describes the results of a more comprehensive experimental activity aimed to the assessment of the effectiveness of an active L-shaped tab to control deep dynamic stall effects that was carried out using an improved system for the L-tab actuation, characterised by a more stiff and accurate manufacturing of the tab. In particular, a wind tunnel test campaign was performed on a oscillating airfoil test rig. Unsteady pressure measurements performed at the airfoil model midspan contour enabled to evaluate the performance of the active L-tab by comparison of the airloads curves evaluated for deep dynamic stall pitching cycles.

2 Experimental set up

The oscillating airfoil test rig is installed in the *S. De Ponte* wind tunnel of Politecnico di Milano. The wind tunnel has a rectangular test section 1.5 m high and 1 m wide with a maximum wind velocity $U_\infty = 55$ m/s and the free stream turbulence level less than 0.1%. A picture of the test rig is presented in Fig. 1. A detailed description of the oscillating airfoil test rig is reported in [15].

The tests activity was carried out over a NACA 23012 airfoil section model, previously investigated by a comprehensive experimental and numerical activity about the characterisation of the fine details of dynamic stall process [16, 17]. The airfoil section model has a $c = 0.3$ m chord and a $b = 0.93$ m span and is pivoted about two external steel shafts with axis at 25% c by a driv-

Figure 1: The oscillating airfoil test rig installed at the *S. De Ponte* wind tunnel of Politecnico di Milano.

ing system composed by a brushless servomotor with a 12:1 gear drive. The model midspan section contour is equipped with 21 pressure taps instrumented with Kulite miniature fast-response pressure transducers (2 PSI F.S.). During the tests, the pressure data were acquired over 60 complete pitching cycles with a sampling rate of 25 kHz. The lift and pitching moment curves were evaluated by the integration of the phase averaged pressures computed using a bin with an amplitude of 0.1° angle of attack. Table 1 presents the positions of the pressure ports on the midspan section contour starting from the leading edge and following a closed loop from the upper to the lower surface of the airfoil. As the last pressure ports on the lower and upper surfaces of the airfoil are located at 90% of the chord, the pressure at airfoil trailing edge was calculated as the mean of the extrapolated functions values obtained using a second order polynomial function interpolating the last three pressure ports signals on the airfoil upper and lower surface, as done in [11].

The layout of the trailing edge L-shaped tab is reported in Fig. 2. The tab spanning the entire airfoil model has a chord of 27 mm. The L-tab is flush with the airfoil upper surface when deployed, so that its end prong behaves similarly to a Gurney flap, even if it is perpendicular to the airfoil upper surface [6] (see Fig. 2a). In this configuration the end prong of the tab protrudes 4 mm from the trailing edge corresponding to about 1.3% chord of effective height h. On the other hand, when retracted the L-shaped tab features

#	x/c	#	x/c	#	x/c
1	0	8	0.453	15	0.459
2	0.01	9	0.618	16	0.373
3	0.044	10	0.76	17	0.285
4	0.096	11	0.9	18	0.185
5	0.164	12	0.9	19	0.118
6	0.28	13	0.767	20	0.06
7	0.358	14	0.628	21	0.02

Table 1: Pressure ports location on the model midspan section.

an angle 10.9° with the airfoil upper surface behaving as an upward deflected trailing edge flap (see Fig. 2b). As the actuation was made by two linear actuators positioned at the model tips, the L-tab was manufactured from a 1 mm thick steel plate to be stiff enough to obtain the same deployment of the tab end prong along the entire model span, particularly in correspondence of the instrumented midspan section.

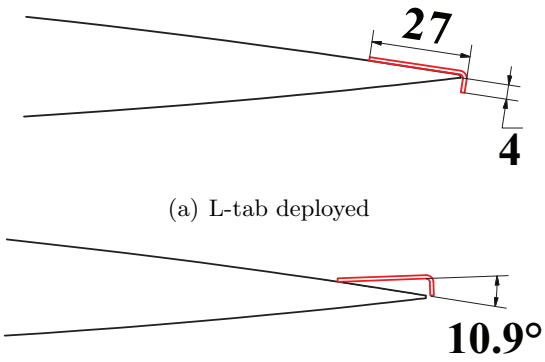

(a) L-tab deployed

(b) L-tab retracted

Figure 2: Layout of the L-shaped tab at the NACA 23012 airfoil trailing edge region (dimensions in mm).

A particular of the actuation system for the L-shaped tab is illustrated in the picture of Fig. 3. The actuation is based on the use of two linear pneumatic actuators with a stroke of 5mm. The micro-cylinders inside the actuators were guided by miniaturized solenoid valves. The actuators move the L-tab acting at the tips of the airfoil model where they are mounted by means of a purposely designed metallic support. This solution enables to avoid any disturbances on the pressure measurements carried out on the model midspan section due to the presence of the actuation sys-

tem. The leading edge of the L-shaped tab is attached on the airfoil model upper surface by means of adhesive tape that behaves as a spanwise hinge.

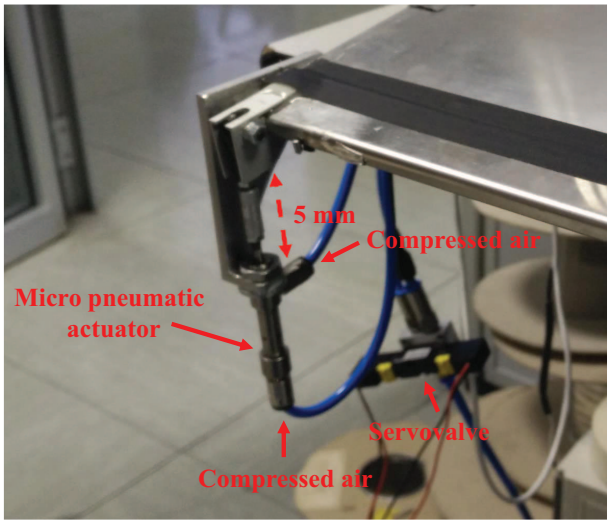

Figure 3: Particular of the actuation system for the L-shaped tab at the airfoil model tip.

The L-tab control along the pitching cycle was carried out by means of an apposite in-house Labview code implementing an open-loop strategy based on digital input-output boards. In particular, a digital board provides the deployed or retracted command signal to the servovalves taking into account both the angular position of the model read from an encoder mounted on the model external shaft and the time delay between the start of the command signal and the complete displacement of the actuator, evaluated by preliminary tests. The assessment of the correct movement of the L-tab during the pitching cycles due to the control system was performed by a preliminary test carried out using two Hall-effect sensors (HES) mounted in correspondence of the midspan section of the model and on a tip section in correspondence of one actuator. Then, during the pressure measurements tests, the HES at midspan section was removed to avoid disturbances, while the HES at tip section was preserved to check the correct deployment and retraction of the L-tab at the angles of attack selected along the pitching cycle for dynamic stall control.

A picture of the airfoil model equipped with the L-tab actuation system inside the wind tunnel test section is presented in Fig. 4.

Figure 4: The NACA 23012 airfoil model equipped with the L-shaped tab in the wind tunnel test section.

3 Results

The effects of the active controlled L-shaped tab were investigated for two deep dynamic stall conditions [1], consisting in a sinusoidal pitching cycle characterised by a mean angle of attack of $\alpha_m = 10°$ and $15°$, respectively, with constant oscillation amplitude of $\alpha_a = 10°$ and reduced frequency k equal to 0.1. The wind tunnel free-stream velocity during the tests was $U_\infty = 30$ m/s, corresponding to a Reynolds number $Re = 6 \times 10^5$ and a Mach number $M = 0.09$.

	Pitching cycle	$\alpha = 10° + 10° \sin(\omega t)$
Case	L-tab Deployed	L-tab Retracted
1	$0° < \alpha < 20°$ up	$20° < \alpha < 0°$ dwn
2	$0° < \alpha < 19°$ up	19° up $< \alpha < 0°$ dwn

	Pitching cycle	$\alpha = 15° + 10° \sin(\omega t)$
Case	L-tab Deployed	L-tab Retracted
3	$5° < \alpha < 25°$ up	$25° < \alpha < 5°$ dwn
4	$5° < \alpha < 23°$ up	23° up $< \alpha < 5°$ dwn

Table 2: Active control parameters for the tests with the L-tab.

Table 2 shows the parameters of the active L-tab control performed during the tests and the denomination of the test cases that will be compared in the following. As can be observed, the test matrix of the wind tunnel campaign included the cases with the L-tab actuated with 50% duty cycle (deployed on the whole upstroke and retracted on the whole downstroke, case 1 and 3) and cases with

the L-tab retracted in upstroke before the top of the motion (case 2 and 4). For a proper evaluation of the L-tab effects on the airfoil performance, the measurements for the clean airfoil configuration were carried out just removing the L-tab but preserving the actuation system at the model tips.

The comparison of the lift and quarter chord pitching moment coefficients curves evaluated respectively for the pitching cycle characterised by $\alpha_m = 10°$ and $\alpha_m = 15°$ is presented in Fig. 5 and 6. The standard deviation of the airloads coefficients are plotted on the airloads coefficients curves.

The tests results show that the deployment of the L-shaped tab produces in upstroke an apparent increase of lift with respect to the clean airfoil configuration for both the pitching cycles considered. This effect is typical of Gurney flaps [9]. In particular, for the pitching cycle characterised by $\alpha_m = 10°$, a maximum increase of about 12% of the lift coefficient was measured at the top of the upstroke motion for the active controlled case 1 (see Fig. 5a).

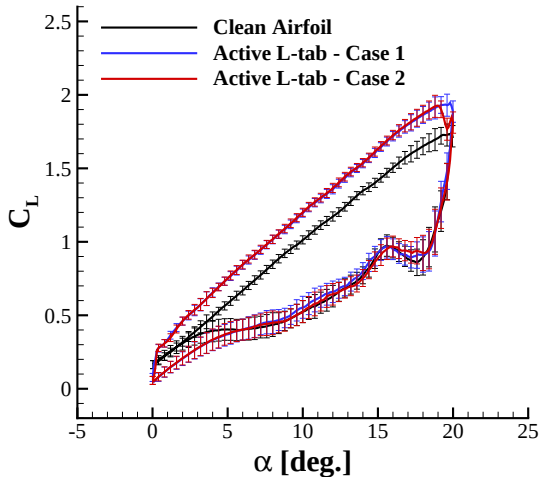

(a)

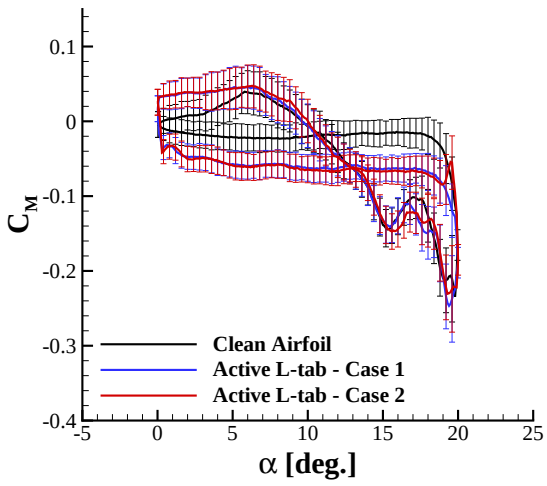

(b)

Figure 5: Comparison of the airloads curves measured for $\alpha = 10° + 10° \sin(\omega t)$, $k = 0.1$ (Re $= 6 \times 10^5$ and M $= 0.09$).

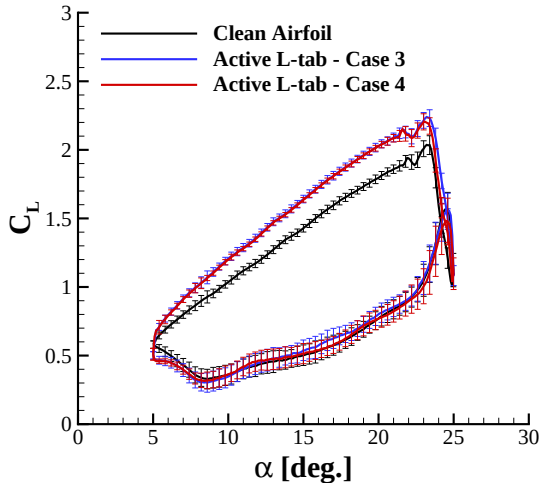

(a)

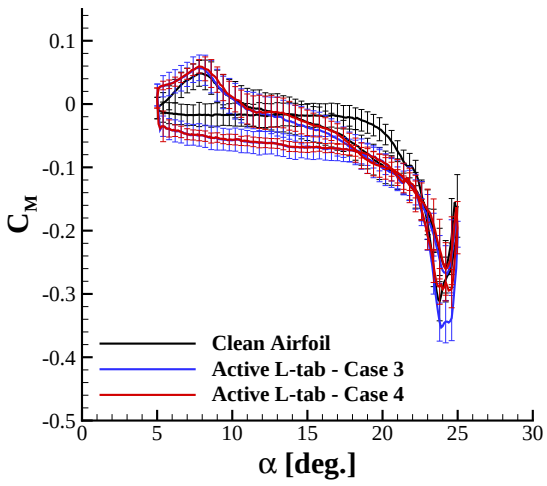

(b)

Figure 6: Comparison of the airloads curves measured for $\alpha = 15° + 10° \sin(\omega t)$, $k = 0.1$ (Re $= 6 \times 10^5$ and M $= 0.09$).

Similarly, for the pitching cycle characterised by $\alpha_m = 15°$, an increase of about 10% is appreciated for the active controlled case 3 in correspondence of the maximum measured lift coefficient (see Fig. 6a). The lift increase produced deploying the L-tab in upstroke can be considered an important benefit for an helicopter rotor blade due to the associated higher level of available thrust very useful on the retreating side of the rotor disk at high advance ratio.

The pitching moment curves comparison shows that the L-tab deployment up to the maximum incidence of the upstroke reached during both the pitching cycles (case 1 and 3) introduces a more severe negative pitching moment peak (see Fig. 5b and 6b). The results of test cases 2 and 4 show that retracting the L-tab before the stall onset produces a reduction of the pitching moment peak of about 2% and 6%, respectively for the pitching cycles with $\alpha_m = 10°$ and $\alpha_m = 15°$.

A quantitative analysis of the two-dimensional aerodynamic damping coefficient calculated according to Carta [18] is presented in Fig. 7 for both the pitching cycles considered. For the pitching cycle characterised by $\alpha_m = 10°$, the net aerodynamic damping calculated for the clean airfoil is negative, as can be clearly deduced by the larger clockwise loop area of the $C_M - \alpha$ curve with respect to the anti-clockwise loop area (see Fig. 5b). On the other hand, both the active controlled test case 1 and 2 produce a quite positive net aerodynamic damping coefficient (see Fig. 7a), as the deployed tab introduces a shift down of the C_M curves while, in the range of angle of attack where the tab is retracted the curve retrace quite well the clean airfoil ones. Consequently, an apparent reduction of the clockwise loop area is obtained with active control, while the anti-clockwise loop area is enlarged with respect to the clean airfoil test condition.

For the pitching cycle characterised by $\alpha_m = 15°$, the net aerodynamic damping coefficient evaluated for the clean airfoil has a slight positive value (see Fig. 7b). The effect of both the active controlled test cases 3 and 4 is to increase tenfold the positive value of the aerodynamic damping coefficient. Thus, the present analysis shows that the use of the active controlled L-tab has to be considered an important benefit for a rotor blade, as it would avoid the risk of stall flutter occurrence.

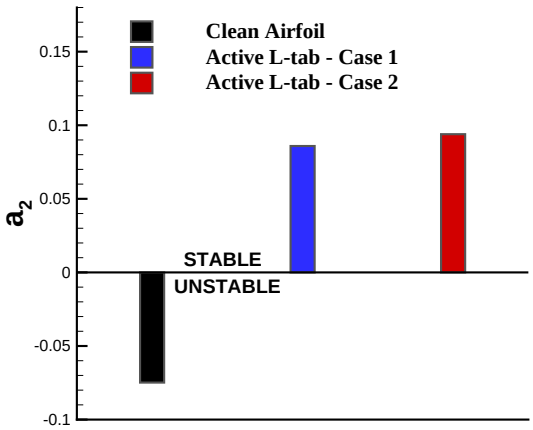

(a) $\alpha = 10° + 10° \sin(\omega t)$

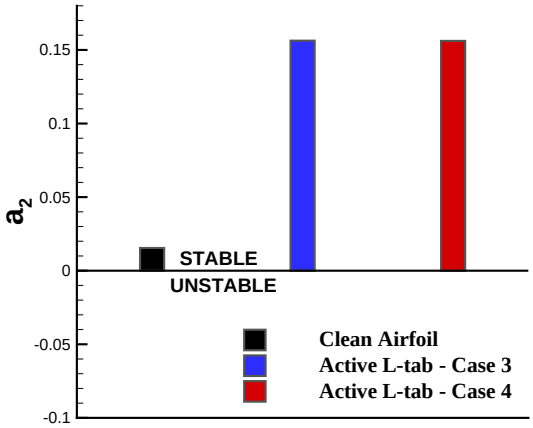

(b) $\alpha = 15° + 10° \sin(\omega t)$

Figure 7: Comparison of the two-dimensional aerodynamic damping coefficient [18].

4 Conclusions

An experimental assessment of the effectiveness of a trailing edge active L-shaped tab for dynamic stall effects control was performed by means of a wind tunnel campaign carried out on a pitching airfoil in deep dynamic stall conditions. The test activity consisted of unsteady pressure measurements to evaluate the sectional aerodynamic loads loops acting on the NACA 23012 airfoil at midspan.

The tests results showed that the control of the active L-tab along the pitching cycle can introduce important advantages for both aerodynamic and

structural performance of the blade. In particular, deploying the tab during almost the whole upstroke motion would produce, analogously to what occurs using a Gurney flap, a conspicuous lift increase corresponding to a higher level of available thrust on the retreating blade. Moreover, the combined L-tab retraction before the stall onset and during the whole downstroke motion would produce an apparent net positive aerodynamic damping related to the pitching moment curve hysteresis that would ensure to avoid the risk of stall flutter occurrence, thus preserving the blade structural integrity. Moreover, a reduction of the pitching moment peak was also observed retracting the L-tab earlier just before stall onset.

The different benefits shown by the present experimental activity encourage a definite assessment of the active L-tab performance in real helicopter operative environment. In fact, this device showed capabilities for dynamic stall control similar to the ones that could be obtained by a deployable Gurney flap but thanks to its design exhibits a better suitability for the use on helicopter blades. Indeed, the L-shaped tab could be easily integrated on the blade external surface, while the actuation system could be stowed inside the blade upstream the trailing edge, where the space requirement are not particularly severe.

References

[1] McCroskey, W.J., The Phenomenon of Dynamic Stall, NASA TM 81264, 1981.

[2] Leishman, J.G., *Principles of helicopter aerodynamics*, Cambridge University Press, 2006.

[3] Gardner, A.D., Richter, K., Mai, H., Neuhaus, D., Experimental Investigation of Air Jets for the Control of Compressible Dynamic Stall, *Journal of the American Helicopter Society*, Vol. 58, N. 4, pp. 1–14, 2013.

[4] Post, M.L., Corke T.C., Separation Control Using Plasma Actuators: Dynamic Stall Vortex Control on Oscillating Airfoil, *AIAA Journal*, Vol. 44, N. 12, pp. 3125-3135, 2006.

[5] Gardner, A.D., Opitz, S., Wolf, C.C., Merz, C.B., Experiment Demonstrating Reduction of Dynamic Stall by a Back-flow Flap, 72nd American Helicopter Society Annual Forum, West Palm Beach, VA, USA, May 17-19, 2016.

[6] Liebeck, R.H., Design of subsonic airfoils for high lift, *Journal of Aircraft*, Vol. 15, pp. 547-561, 1978.

[7] Kentfield, J.A.C., The potential of gurney flaps for improving the aerodynamic performance of helicopter rotors, AIAA International Powered Lift Conference, AIAA Paper 93-4883, 1993.

[8] Yeo, H., Assessment of active controls for rotor performance enhancement, *Journal of the American Helicopter Society*, Vol. 53, N. 2, pp. 152-163, 2008.

[9] Kinzel, M.P., Maughmer, M.D., Duque E.P.N., Numerical investigation on the aerodynamics of oscillating airfoils with deployable gurney flaps, *AIAA Journal*, Vol. 48, N. 7, pp. 1457–1469, 2010.

[10] Woodgate, M., Pastrikakis, V., Barakos, G.N., Method for Calculating Rotors with Active Gurney Flaps, *Journal of Aircraft*, Vol. 53, N. 3, pp. 605–626, 2016.

[11] Chandrasekhara, M., Martin, P., Tung, C., Compressible Dynamic Stall Performance of a Variable Droop Leading Edge Airfoil with a Gurney Flap, *Journal of American Helicopter Society*, Vol. 53, N. 1, pp. 18–25, 2008.

[12] Motta, V., Zanotti, A., Gibertini G., Quaranta, G., Numerical assessment of an L-shaped Gurney flap for load control, *Proceedings of the Institution of Mechanical Engineers, Part G: Journal of Aerospace Engineering*, Vol. 231, N. 5, pp. 951–975, 2017.

[13] Zanotti, A., Grassi, D., Gibertini G., Experimental investigation of a trailing edge L-shaped tab on a pitching airfoil in deep dynamic stall conditions, *Proceedings of the Institution of Mechanical Engineers, Part G: Journal of Aerospace Engineering*, Vol. 228, N. 12, pp. 2371–2382, 2014.

[14] Pisetta, G., Verifica sperimentale degli effetti di un gurney flap attivo su un profilo oscillante in regime di stallo dinamico, *Master's thesis*, Politecnico di Milano, 2016.

[15] A. Zanotti, F. Auteri, G. Campanardi and G. Gibertini. An Experimental Set Up for the Study of the Retreating Blade Dynamic Stall, 37th European Rotorcraft Forum, 13-15 September, Gallarate (VA), Italy, 2011.

[16] Zanotti, A., Gibertini, G., Experimental investigation of the dynamic stall phenomenon on a NACA 23012 oscillating airfoil, *Proceedings of the Institution of Mechanical Engineers, Part G: Journal of Aerospace Engineering*, Vol. 227, N. 9, pp. 1375–1388, 2013.

[17] Zanotti, A., Nilifard, R., Gibertini, G., Guardone, A., Quaranta, G., Assessment of 2D/3D Numerical Modeling for Deep Dynamic Stall Experiments, *Journal of Fluids and Structures*, Vol. 51, pp. 97-115, 2014.

[18] Carta, F.O., An analysis of the stall flutter instability of helicopter rotor blades, *Journal of the American Helicopter Society*, Vol. 9, pp. 1-8, 1967.